HIV

Quality and quantity of T_{FH} cells are critical for broad antibody development in $SHIV_{AD8}$ infection

Takuya Yamamoto,[1]* Rebecca M. Lynch,[2]* Rajeev Gautam,[3] Rodrigo Matus-Nicodemos,[1] Stephen D. Schmidt,[2] Kristin L. Boswell,[1] Sam Darko,[4] Patrick Wong,[2] Zizhang Sheng,[5] Constantinos Petrovas,[1] Adrian B. McDermott,[1] Robert A. Seder,[6] Brandon F. Keele,[7] Lawrence Shapiro,[5] Daniel C. Douek,[4] Yoshiaki Nishimura,[3] John R. Mascola,[2] Malcolm A. Martin,[3] Richard A. Koup[1†]

Broadly neutralizing antibodies (bNAbs) protect against HIV-1 infection, yet how they are generated during chronic infection remains unclear. It is known that T follicular helper (T_{FH}) cells are needed to promote affinity maturation of B cells during an immune response; however, the role of T_{FH} during HIV-1 infection is undefined within lymph node germinal centers (GCs). We use nonhuman primates to investigate the relationship in the early stage of chronic $SHIV_{AD8}$ (simian-human immunodeficiency virus AD8) infection between envelope (Env)–specific T_{FH} cells, Env-specific B cells, virus, and the generation of bNAbs during later infection. We found that both the frequency and quality of Env-specific T_{FH} cells were associated with an expansion of Env-specific immunoglobulin G–positive GC B cells and broader neutralization across HIV clades. We also found a correlation between breadth of neutralization and the degree of somatic hypermutation in Env-specific memory B cells. Finally, we observed high viral loads and greater diversity of Env sequences in rhesus macaques that developed cross-reactive neutralization as compared to those that did not. These studies highlight the importance of boosting high-quality T_{FH} populations as part of a robust vaccine regimen aimed at eliciting bNabs.

INTRODUCTION

Most anti–HIV-1 broadly neutralizing antibodies (bNAbs) show a high degree of somatic hypermutation (SHM) (*1*), suggesting that they have undergone extensive affinity maturation within germinal centers (GCs). Specialized follicular helper CD4 T (T_{FH}) cells support the formation of GCs and contribute to B cell differentiation, isotype switching, SHM, and the survival of high-affinity memory B cells and plasma cells through secretion of cytokines and chemokines [IL-4 (interleukin-4), IL-21, and CXCL13] and interactions with GC B cells via costimulatory receptors (*2*–*5*). T_{FH} cells are characterized by high expression of Bcl6, CXCR5, and costimulatory receptors (PD-1 and ICOS) and low expression of CCR7. Simian immunodeficiency virus (SIV) infection of rhesus macaques (RMs) alters the CD4 T cell dynamic in lymph nodes (LNs), leading to T_{FH} cell accumulation and increased egress of non-T_{FH} cells (*3*). This accumulation of T_{FH} cells is associated with increased frequency of activated GC B cells in LN and SIV-specific antibodies in plasma. However, a direct role of T_{FH} cells in eliciting broadly neutralizing responses against HIV remains unclear, and a deeper understanding may lead to new ways of analyzing vaccine potential in nonhuman primates.

Simian-human immunodeficiency virus AD8 ($SHIV_{AD8}$) consistently establishes sustained viremia, causes unremitting depletion of CD4 T cells, and induces clinical immunodeficiency and death in inoculated RMs (*6*). Many of the pathologic and immunologic consequences of HIV-1 infection can be observed in RMs infected with $SHIV_{AD8}$ (*6*). In particular, potent cross-clade NAbs against tier 1 and tier 2 HIV-1 isolates can be generated in some $SHIV_{AD8}$-infected RMs (*7*–*9*).

Here, we investigated the relationship between the generation of broader cross-clade neutralizing activity and aspects of T_{FH} cells, envelope (Env)–specific B cells, and viral replication during $SHIV_{AD8}$ infection. We found that the frequency of Env-specific T_{FH} cells and Env-specific immunoglobulin G–positive (IgG^+) GC B cells within the LN correlated with the subsequent development of NAbs in the chronic phase of infection. We also found that Env-specific T_{FH} cells in monkeys with greater neutralizing activity expressed a gene profile skewed toward T_{FH} and away from T helper 1 (T_H1) cells. Broader antibody neutralization was also associated with greater affinity maturation in memory B cells.

RESULTS

Longitudinal analysis of T_{FH} cells and neutralization breadth in $SHIV_{AD8}$-infected macaques

Eight RMs were inoculated intrarectally with $SHIV_{AD8}$. All developed persistent infection (set point viremia: 10^2 to $>10^5$ RNA copies/ml) (Fig. 1A), and all but one had a gradual loss of total circulating CD4 T cells (Fig. 1B). We first determined the frequency of T_{FH} cells in the LN of SHIV-infected RMs (*3*, *10*, *11*). The $CD28^{dim}CD95^{low}$ (hereafter referred to as naïve) CD4 T cells were used to set gates for the identification of particular populations within the $CD28^{high}CD95^{high}$ [hereafter referred to as central memory (CM)] compartment (fig. S1). CM CD4 T cells expressing a $CXCR5^+PD\text{-}1^{++}$ phenotype were defined as T_{FH} cells for further analyses. We observed variable accumulation of T_{FH} cells in LN tissues beginning at 20 weeks and extending through 44 to 47 weeks post-infection (PI)

[1]Immunology Laboratory, Vaccine Research Center, National Institute of Allergy and Infectious Diseases (NIAID), National Institutes of Health (NIH), Bethesda, MD 20892, USA. [2]Humoral Immunology Section, Vaccine Research Center, NIAID, NIH, Bethesda, MD 20892, USA. [3]Laboratory of Molecular Microbiology, NIAID, NIH, Bethesda, MD 20892, USA. [4]Human Immunology Section, Vaccine Research Center, NIAID, NIH, Bethesda, MD 20892, USA. [5]Department of Biochemistry and Molecular Biophysics, Columbia University, New York, NY 10032, USA. [6]Cellular Immunology Section, Vaccine Research Center, NIAID, NIH, Bethesda, MD 20892, USA. [7]AIDS and Cancer Virus Program, Leidos Biomedical Research Inc., Frederick National Laboratory for Cancer Research, Frederick, MD 21702, USA.
*These authors contributed equally to this work.
†Corresponding author. E-mail: rkoup@mail.nih.gov

(4.60 to 41.3%, Fig. 1C). We next assessed whether the accumulation of T_{FH} cells in LN was associated with general immune activation. The level of plasma soluble CD14 (sCD14), a marker of immune activation (*12*), was significantly higher at 44 to 47 weeks PI compared to before infection ($n = 8$; $P = 0.0234$, Wilcoxon matched-pairs signed rank test; fig. S2A). We also found that IL-6, a proinflammatory cytokine that is a critical regulator of T_{FH} cells (*3*, *13*, *14*), was increased at 20 weeks, substantially earlier than sCD14 (fig. S2B).

$SHIV_{AD8}$-infected RMs have been reported to develop cross-reactive NAbs between 34 and 50 weeks PI (*7*, *8*). We assessed neutralizing activity in plasma from all eight monkeys at multiple time points and found that neutralization activity against the related HIV-1 strain ADA arose between 44 and 47 weeks PI (Fig. 1D and fig. S3A). To quantify the breadth and potency of the plasma neutralization activity, we assigned points based on ID_{50} (50% inhibitory dilution) titers (one point for titers between 40 and 99, two points for titers between 100 and 999, and three points for titers ≥1000) for each virus in a multiclade 19-virus panel. We added these points together for an overall neutralization score. We observed a range of neutralization scores at 44 to 47 weeks PI (Fig. 1E), with some RMs developing reasonably broad cross-clade responses (some against tier 2 HIV-1) by weeks 97 to 125 (fig. S3B). The neutralization score is treated as a continuous variable throughout the article, but for ease of visualization, the top three neutralizers are indicated in red, the middle three in blue, and the lowest two in black in all figures.

Generation of Env-specific T_{FH} cells and GC B cells during $SHIV_{AD8}$ infection

B cell receptor (BCR) affinity maturation is dependent on T_{FH} and antigen-specific B cell interactions in the GCs of LNs. We therefore determined the frequency of GC B cells in LN and memory B cells in peripheral blood

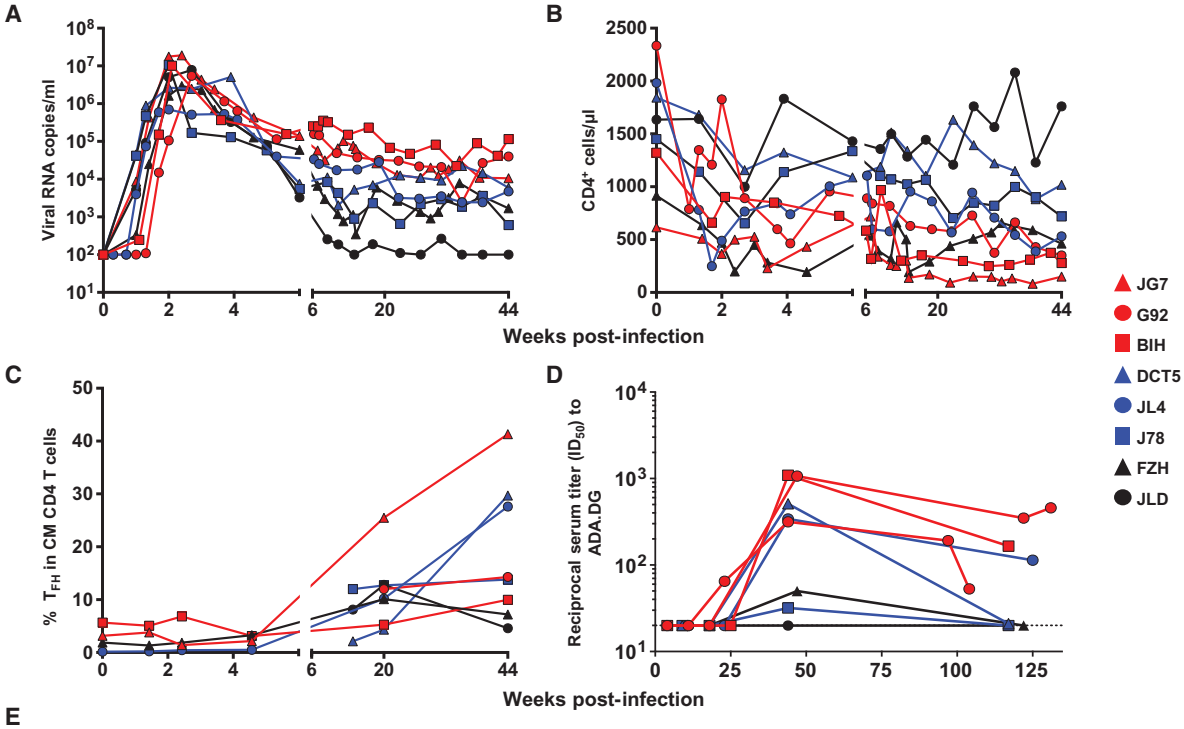

E

Clade/type		A			02_AG	B									C		Other			
Animal ID	Weeks post infection	Q23.17	RW020.2	UG037.8	DJ263.8	6535.3	7165.18	AC10.0.29	ADA	BaL.01	HXB2	CAAN.A2	JR-CSF	JR-FL	SS1196.1	MW965.26	ZM109.4	$SHIV_{DH12}$ clone 7 V3 AD8	$SHIV_{AD8}$ CK15 3-3	SIVmac 251.30. SIV	Neut score
JG7	47	16	17	<10	102	45	<10	<10	1068	286	1344	54	290	1060	198	5287	11	3283	149	<10	27
BIH	44	<10	<10	<10	441	98	<10	<10	1091	384	5847	<10	1601	11	529	20,943	<10	3965	14	<10	22
G92	44	<10	<10	<10	53	116	<10	<10	316	235	5259	<10	88	237	172	1717	<10	1377	44	<10	22
DCT5	44	10	<10	<10	37	123	<10	<10	512	248	8958	<10	949	15	915	3021	<10	2777	<10	<10	19
JL4	44	<10	<10	<10	109	52	<10	<10	342	51	1519	<10	70	15	100	9819	<10	1413	28	<10	18
J78	44	<10	<10	<10	38	56	<10	<10	32	193	3265	<10	258	<10	507	968	<10	3869	<10	<10	15
FZH	47	<10	<50	<10	<10	<10	<10	<50	<50	33	915	<10	<50	<10	42	1546	<10	1724	<10	<10	9
JLD	44	<10	<10	<10	<10	13	<10	<10	16	14	891	<10	<10	<10	26	63	<10	132	<10	<10	5

Fig. 1. Longitudinal development of T_{FH} and B cell responses after $SHIV_{AD8}$ infection. (**A** to **D**) Levels of plasma viremia (A), absolute numbers of peripheral $CD4^+$ T cells (B), total frequency of T_{FH} cells within the LN CM CD4 population (C), and serum titers against HIV-1 ADA (D) over time of infection. (**E**) ID_{50} neutralization titers against a 19-virus panel including $SHIV_{DH12}$, $SHIV_{AD8\text{-}EO}$, the indicated clade A, B, and C HIV-1 isolates, and the negative control SIVmac251.30 for week 44 to 47 PI sera. Values between 40 and 99 are shown in green; values between 100 and 999 are shown in yellow; and values ≥1000 are shown in red. Neutralization scores are the sum of the neutralization activity against each isolate (red is 3, yellow is 2, and green is 1). To visually distinguish neutralization patterns, RMs with top scores are indicated in red, intermediate are in blue, and low scores are in black.

mononuclear cells (PBMCs) throughout infection and quantified HIV Env-specific IgG$^+$ GC B cells, which we were able to detect after 20 weeks PI (fig. S4). We focused on the week 44 to 47 time points because this is the time point when neutralization activity is detected in all RMs (fig. S3A). At this time, we observed a significant correlation between the frequency of total T_{FH} cells and total IgG$^+$ GC B cells in LN (n = 8; P = 0.0494, r = 0.5013, Spearman rank test; fig. S5A) but no correlation between total T_{FH} cells in LN and total IgG$^+$ memory B cells in PBMCs (fig. S5B). To investigate the antigenic specificity of these cells, we quantified HIV Gag and Env-specific T_{FH} cells [by CD154, IL-4, or IFNγ (interferon γ) expression] in LNs (fig. S6A). Both Gag- and Env-specific T_{FH} cells were detectable in LNs at 44 to 47 weeks PI (fig. S6B).

We further analyzed the relationship between the frequencies of Env-specific T_{FH} cells and Env-specific IgG$^+$ GC B cells and the neutralization scores in the $SHIV_{AD8}$-infected RMs. The frequency of Gag-specific CD154$^+$ or IFNγ$^+$ T_{FH} cells tended to be greater than that of Env-specific T_{FH} cells, although there was no clear difference in the frequency of IL-4$^+$ T_{FH} cells between these two specificities (fig. S6B). We were unable to assess IL-21 expression in these LN samples because of unreliable staining using available reagents. Nevertheless, we found that the frequency of CD154$^+$ and IL-4$^+$, but not IFNγ$^+$, Env-specific T_{FH} cells, strongly correlated with Env-specific IgG$^+$ GC B cells (n = 8; P = 0.0198, r = 0.6231 and P = 0.0079, r = 0.7181, respectively, Spearman rank test; Fig. 2A). There was no correlation between Gag-specific T_{FH} responses and the frequency of Env-specific IgG$^+$ GC B cells (fig. S7A). These results strongly suggest that Env-specific T_{FH} cells, especially those producing IL-4, are necessary for the generation or maintenance of Env-specific IgG$^+$ GC B cells during the chronic phase of $SHIV_{AD8}$ infection.

Immunological correlates of bNAb responses

Next, we found significant correlations between neutralization scores at weeks 44 to 47 and the frequency of Env-specific CD154$^+$ (n = 8; P = 0.0288, r = 0.5769, Spearman rank test) and IL-4$^+$ (n = 8; P = 0.0104, r = 0.6922, Spearman rank test) T_{FH} cells, but not IFNγ$^+$ T_{FH} cells (Fig. 2B) at the same time points. Furthermore, we found that this correlation remained between later neutralization scores at weeks 97 to 125 and the frequency of Env-specific CD154$^+$ (n = 8; P = 0.0033, r = 0.7871, Spearman rank test) and IL-4$^+$ (n = 8; P = 0.0008, r = 0.8676, Spearman rank test) T_{FH} cells at weeks 44 to 47 (fig. S7B). We also found a strong correlation between the frequency of Env-specific IgG$^+$ GC B cells in LNs and both early [weeks 44 to 47 (n = 8; P = 0.0015, r = 0.8368, Spearman rank test)] and later [weeks 97 to 125 (n = 8; P = 0.0187, r = 0.6301, Spearman rank test)] neutralization scores (fig. S7C). Therefore, not all phenotypically defined Env-specific T_{FH} cells are equal because those that produce IL-4, but not those that produce IFNγ, appear to coincide with the development of Env-specific IgG$^+$ GC B cells as well as neutralizing responses against HIV.

Molecular signature of gene expression in Env-specific T_{FH} cells

To further define the characteristics of effective T_{FH} cells, we first confirmed the expression levels of Bcl6 in T_{FH} cells by flow cytometry (Fig. 3A and fig. S8). Compared to other CD4 T cell populations such as naïve or non-T_{FH} CM cells, the expression of Bcl6 is highest in T_{FH} cells (Fig. 3B). We next analyzed the relative gene expression of multiple T cell–associated transcription factors, cytokines, and chemokines in CD154$^+$ Env-specific T_{FH} cells in the RMs (*2*, *3*, *15*). We found that

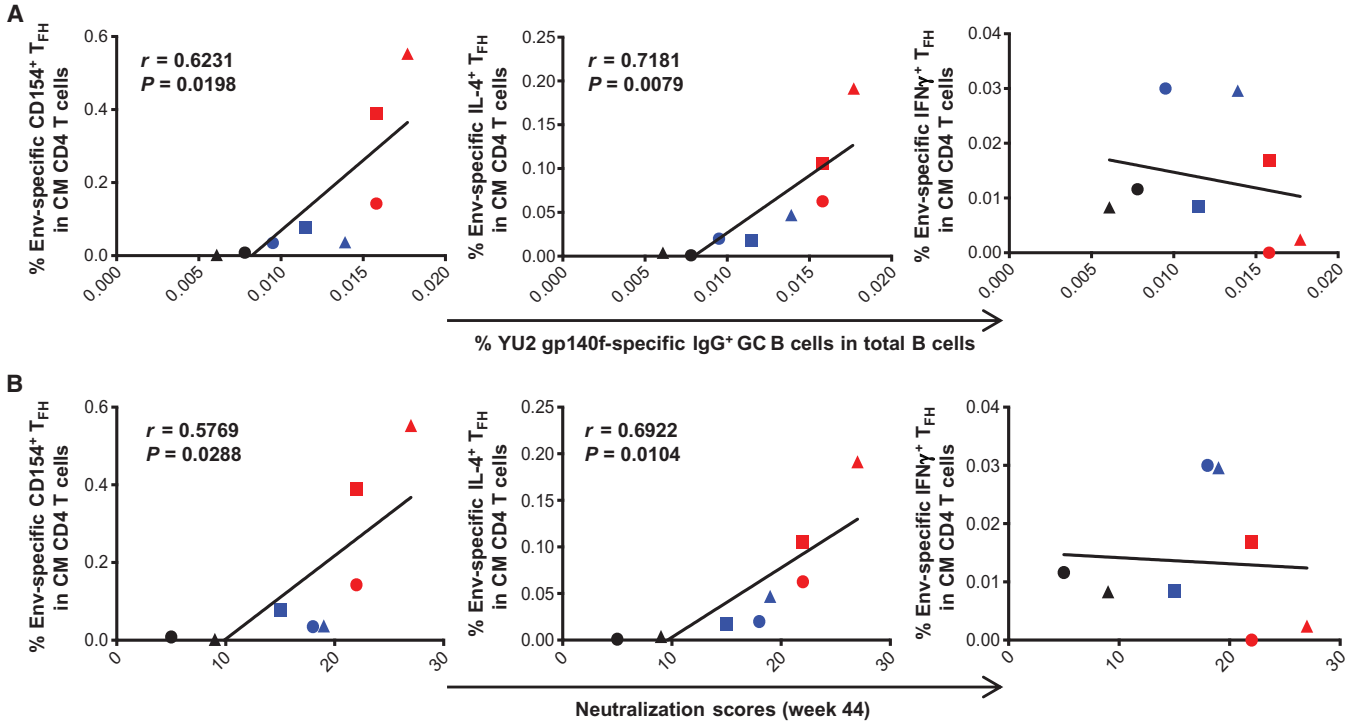

Fig. 2. Antigen-specific responses in the LN. (**A**) Percentage of ConB Env-specific CD154$^+$, IL-4$^+$, and IFNγ$^+$ T_{FH} cells as a function of the percentage of YU2 gp140f-specific IgG$^+$ GC B cells at week 44. Lines indicate correlations determined by linear regression analysis (n = 8 for all graphs). (**B**) Percentage of ConB Env-specific CD154$^+$, IL-4$^+$, and IFNγ$^+$ T_{FH} cells as shown as a function of week 44 to 47 PI neutralization scores.

Env-specific T_{FH} cells expressed higher levels of *Bcl6, MAF, MYB, IL-21,* and *CXCL13* and a lower level of IFNγ compared to the non-T_{FH} CM cells (fig. S9A). The expression of *PRDM1* (*Blimp-1*) was not significantly different between non-T_{FH} CM cells and Env-specific T_{FH} cells. We further elucidated differences in populations by quantifying the expression levels of transcription factors related to T_H1 [*TBX21* (*T-bet*)], T_H2 (*GATA3*), T_H17 (*RORC*), and T_{reg} (T regulatory) (*Foxp3*) cells. There was no significant difference in *TBX21, GATA3, RORC,* and *Foxp3* between non-T_{FH} CM cells and Env-specific T_{FH} cells (fig. S9B). To confirm the relevance of mRNA expression as measured by quantitative reverse transcription polymerase chain reaction (qRT-PCR), we further quantified protein expression levels by flow cytometry for four main transcription factors. There was a robust correlation between mRNA and protein expression (fig. S9C). We then performed a clustering analysis of mRNA expression in T_{FH} cells from each RM, and we detected a clear difference in Env-specific T_{FH} cell gene expression between RMs with high (JG7, G92, and BIH) versus poor (FZH and JLD) neutralization scores (Fig. 3C). The expression of T_{FH}-related genes (*Bcl6, MAF, MYB, CXCL13,* and *IL-21*) and the T_H2-type gene (*GATA3*) were higher in RM with cross-reactive neutralizing responses as compared to those with poor or intermediate neutralizing responses. There was also a shift from a typical T_{FH} cell gene expression profile to a more heterogeneous gene expression profile in these latter RMs. The expression of *Foxp3* was lower in RM with high compared to low neutralization scores. These results indicate that the generation of broad neutralizing responses is associated with a distinct population of Env-specific T_{FH} cells.

Development of cross-reactive neutralization activity and affinity-matured B cells

Production of cytokines IL-21 and IL-4 by T_{FH} cells drives affinity maturation of BCRs within GCs (*16*–*18*). We therefore measured the level of SHM in the heavy chain variable gene (V_H) of single cell–sorted Env-specific IgG^+ B cells from bone marrow (BM) at weeks 44 to 47 PI. The whole variable region of heavy chains was PCR-amplified from individual Env-specific B cells and compared to a new database of RM V_H gene germline sequences (*19*). There was a large expansion of V_H4 family BCRs within all RMs (fig. S9), a finding that may partially reflect the preferential usage of V_H4 in RM class-switched IgG B cells (*20*). Overall, SHM accounted for between 0 and 18% of the nucleotides in the V_H genes (Fig. 4A). RMs with higher neutralization scores had fewer BCRs with low mutation rates (between 0 and 5%), but all RMs had expanded clonal families (fig. S10). The mean level of SHM per animal correlated with both the magnitude of $IL\text{-}4^+$ Env-specific T_{FH} cells (Fig. 4B) and neutralization score of the RMs over time (Fig. 4C). These data provide additional evidence of a link between degree of affinity maturation in memory B cells and ability to neutralize diverse strains of HIV.

To confirm that highly matured B cells were contributing to plasma neutralization, we cloned six of the identified YU2 gp140f-sorted BCRs from JG7, the RM that developed the broadest neutralizing response. These monoclonal antibodies (mAbs) represented three independent clonal families of highly mutated B cells (fig. S11A), and one family (JG7-VRC30) had an exceptionally long CDRH3 of 31 amino acids according to IMGT (international ImMunoGeneTics information system) definition (*21*) (fig. S11B). Of these mAbs, only the four cloned from the JG7-VRC30 family were cross-neutralizing, and these affinity-matured antibodies recapitulated the tier 1 and 1B, but not the tier 2, plasma neutralizing activity (fig. S11C). Their neutralization profile was similar to that of the CD4-induced (CD4i) antibody 17b, and mapping data confirmed co-receptor specificity. Binding by these mAbs to gp120 was knocked down in the presence of an I420R mutation in the co-receptor binding site (fig. S12A), and they competed with 17b for binding to gp120 and increased binding of CD4-Ig to gp120 (fig. S12B). 17b is a human antibody with a long, acidic, tyrosine-rich CDRH3 that is directed against the co-receptor binding site of HIV-1 (*22*), and this VRC30 family of antibodies appears to be the same type of antibody but originating in an SHIV-infected RM. Furthermore, these data corroborate that a highly mutated antibody lineage to a CD4i epitope contributes to some, but not all, plasma cross-reactivity at this time PI.

Diversity of viral sequences

We next evaluated the relationship between viral loads and neutralization scores. We found that set point viral load (the mean of $\log_{10}$ viral loads from 8 to 44 weeks PI) correlated with neutralization score throughout infection (Fig. 5A). Specifically, although neutralization scores slightly fluctuated, the RMs with the highest set point viral load had the highest neutralization scores at early (week 44) and later (week 120) times PI.

To examine viral diversity within the quasispecies, we performed single-genome amplification and *env* sequencing on longitudinal plasma samples from seven of the eight RMs. The gp160 sequences were aligned to the *env* gene of the transmitted/founder $SHIV_{AD8\text{-}EO}$ molecular clone (T/F), and maximum likelihood trees were constructed. Although most RMs had genetically homogeneous sequences early in infection (weeks 2 to 8), by week 8, viral diversity appeared evident in RMs with higher viral loads. It was not possible to sequence viral *env* genes in all RMs at all time points, especially those with low viral loads. Nevertheless, these phylogenetic trees highlight that the greatest viral evolution occurred in the RMs with the highest viral load set point and highest neutralization scores (Fig. 5B). T_{FH} cell and antibody neutralizing activity were detected between weeks 20 and 44 PI, which means that viral diversity appears to precede this development, because it was apparent in some RMs by 8 weeks PI. Furthermore, it is interesting to note that in the one RM with the highest neutralization score throughout infection, JG7, viral evolution appeared linear over time as compared to the increased branching seen in other monkeys' viral evolution. Overall, these data concur with findings in HIV-1 infection that viral set point, viral load, early *env* diversity, and time from infection all correlate with the development of neutralization breadth (*23*–*25*).

DISCUSSION

Interaction of T_{FH} and B cells in GCs is required for the orderly development and maturation of an antibody response (*2*, *4*, *5*). Both HIV and SIV affect multiple aspects of this interaction, thereby altering the antibody response. Specifically, they infect and alter the dynamics, function, and transcriptional profile of T_{FH} cells (*3*, *10*, *11*, *26*). Additionally, immune activation associated with infection can affect the cytokine and chemokine milieu of the GC where these critical interactions occur (*3*). Although many changes in peripheral B cell and antibody responses have been described in HIV infection (*27*, *28*), how the altered interactions within the GCs affect the development of broad serum neutralization remains unclear. It has been observed that HIV infection induces a continuum of bNab responses (*23*, *29*), but the causative factors have not previously been delineated.

Infection of RMs with $SHIV_{AD8}$ provides an ideal system in which to study the induction of cross-reactive neutralizing responses (*6*–*8*), and development of neutralizing activity against two specificities (co-receptor and N332 supersite of vulnerability) has now been demonstrated (*8*). In this model, we observed 13 variables that are highly correlated in a clustering analysis, including quality and quantity of T_{FH} and GC B cells, viral set point, and neutralization score, and negatively correlated with non-T_{FH} transcription factors such as FOXP3 and TBET (Fig. 6 and table S1). Total T_{FH} cells and IgG^+ GC B cells are not included in this cluster 1, suggesting that an increase in the frequency of total T_{FH} cells is not sufficient to elicit breadth. This accumulation of total T_{FH} cells could, by maintaining increased numbers of GC B cells, contribute to B cell abnormalities while also serving as a major target and source of progeny virions (*11*). Alternatively, infection of T_{FH} cells may produce the chronic Env antigen required to drive the GC reaction and lead to SHM within Env-specific B cells. Consistent with previous studies (*10*), we found

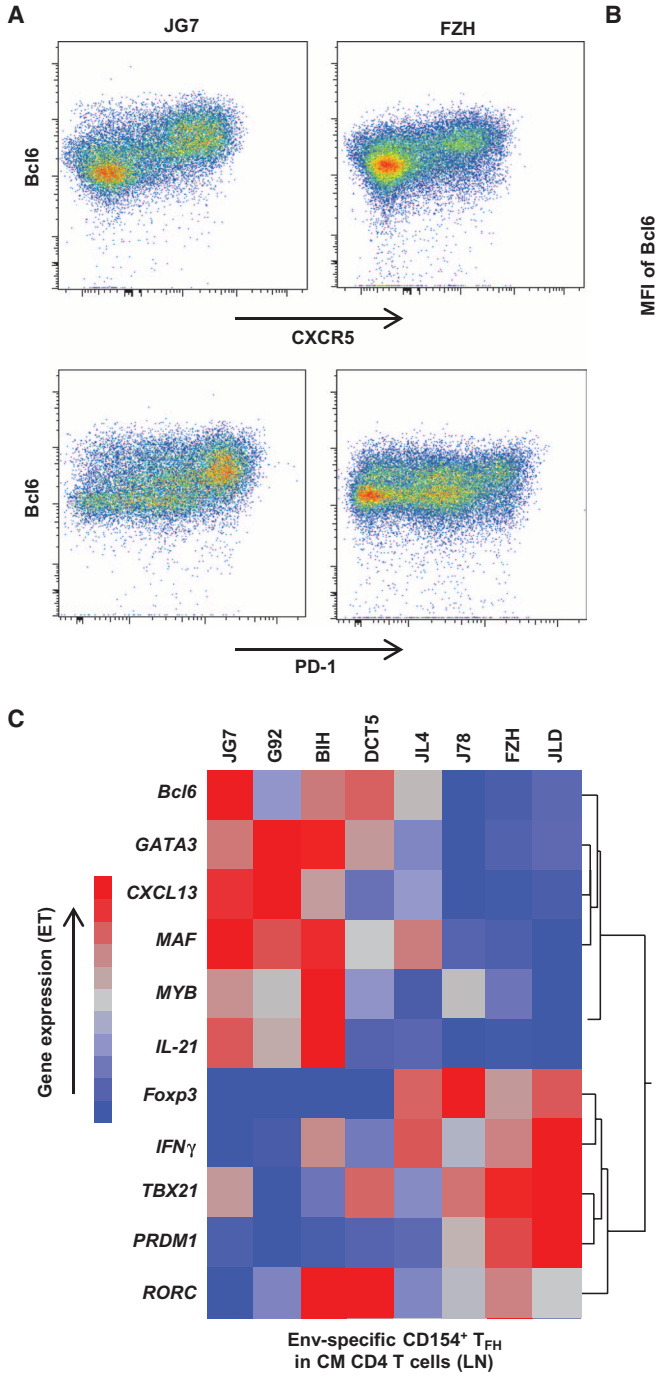

Fig. 3. Molecular signature of antigen-specific CD154 T_{FH} cells that correlate with neutralization. (**A**) Gating strategy for expression of transcription factor Bcl6 and T_{FH} markers CXCR5 and PD-1. (**B**) Mean fluorescence expression of Bcl6 within each naïve, non-T_{FH}, and T_{FH} [as measured by CXCR5 and PD-1 expression (fig. S1)] populations of CD4 T cells within each RM. MFI, mean fluorescence intensity. (**C**) Gene signatures of Env-specific $CD154^+$ T_{FH} cells. LN cells were stimulated with Env peptide pools for 3 hours and sorted according to CXCR5, PD-1, and CD154 expression. Unsupervised two-way hierarchical clustering analysis is shown on the basis of standardized data of expression threshold (ET) values for each gene. The ranges of ET values for each gene are the following: *Bcl6*, 3.56 to 18.46; *GATA3*, 0.21 to 5.81; *CXCL13*, 5.97 to 17.58; *MAF*, 7.5 to 11.99; *MYB*, 1.26 to 5.03; *IL-21*, 0 to 17.82; *Foxp3*, 0 to 2.89; *IFNγ*, 2.08 to 11.04; *TBX21*, 2.68 to 5.42; *PRDM1*, 1.16 to 28.12; and *RORC*, 4.25 to 10.47.

Gag- and Env-specific T_{FH} responses in LNs and also found correlations between Env-specific T_{FH} responses, Env-specific IgG^+ GC B cells, and neutralization scores. Whereas it has been reported that T_{FH} cell dysfunction impairs B cell immunity during HIV-1 infection (*26*), our data strongly suggest that the maintenance of Env-specific T_{FH} cells, especially IL-4–producing Env-specific T_{FH} cells, and Env-specific IgG^+ GC B cells is necessary for generating broader NAbs. It is possible that IL-4 influences the isotype of the antibody during class switching or that IL-4 aids in the development of the T_{FH} program.

A caveat to our findings is the limited number of macaques with which to conduct these experiments. Therefore, we were careful to not draw any conclusions based on any single macaque but rather all eight macaques as a continuum.

T_{FH} cells are highly polyclonal in GCs, control the number of B cell divisions per GC cycle, and also regulate BCR hypermutation (*18*, *30*). GCs contain not only classical T_{FH} cells but also CD4 follicular regulatory T (T_{FR}) cells (*31*). We observed higher expression of T_{FH}-related genes in the $CD154^+$ Env-specific T_{FH} cell population in RMs that developed neutralizing activity against multiple HIV clades as compared to those who did not. It is possible that the lack of persistent antigen and low Bcl6 expression during infection in these low neutralizing RMs explain this skewing (*32*–*34*). The expression of Bcl6 may antagonize the development of a T_H1 or alternatively may be a result of a less-developed T_{FH} phenotype in the low viremic animals. This finding indicates that not all T_{FH} cells are the same and that induction of phenotypically defined T_{FH} with a transcriptional profile skewed toward T_{FH} and away from T_H1 and T_{FR} is required to drive affinity maturation of the B cell response. Therefore, both quantity and quality of Env-specific T_{FH} cells are important for maintaining Env-specific IgG^+ GC B cells and eliciting broader antibodies.

Very few chronically infected individuals develop exceptional breadth, and an explanation for this rarity remains elusive. Previous reports have found that frequency of circulating memory T_{FH} cells, length of HIV-1 infection, and level of plasma viremia are all associated with the development of breadth (*23*, *24*, *35*, *36*), in particular set point viral load and early *env* gene diversity (*25*). Most HIV-specific bNAbs isolated from these special donors have high levels of SHM and/or long CDRH3s (*37*). The B cells that produce these highly mutated antibodies are, by necessity, the products of multiple rounds of affinity maturation within GCs, leading to the generation of long-lived memory B cells or memory plasma cells that home to the BM (*38*). Here, we analyzed early samples from <1 year PI, during which time modest cross-reactivity had developed. We observed higher levels of SHM in the V_H genes of BM Env-specific IgG^+ memory B cells in RMs that developed broader NAb responses as compared to those who did not. Furthermore, we found a correlation between SHM, Env-specific T_{FH} cells, and viral load set point. The fact that mAbs recapitulating some of the serum neutralizing activity were identified and showed extensive SHM confirms that highly affinity-matured B cells are contributing to the observed neutralization breadth. Epitope mapping of these mAbs also highlights the fact that these BCRs must go through affinity maturation against sites of vulnerability

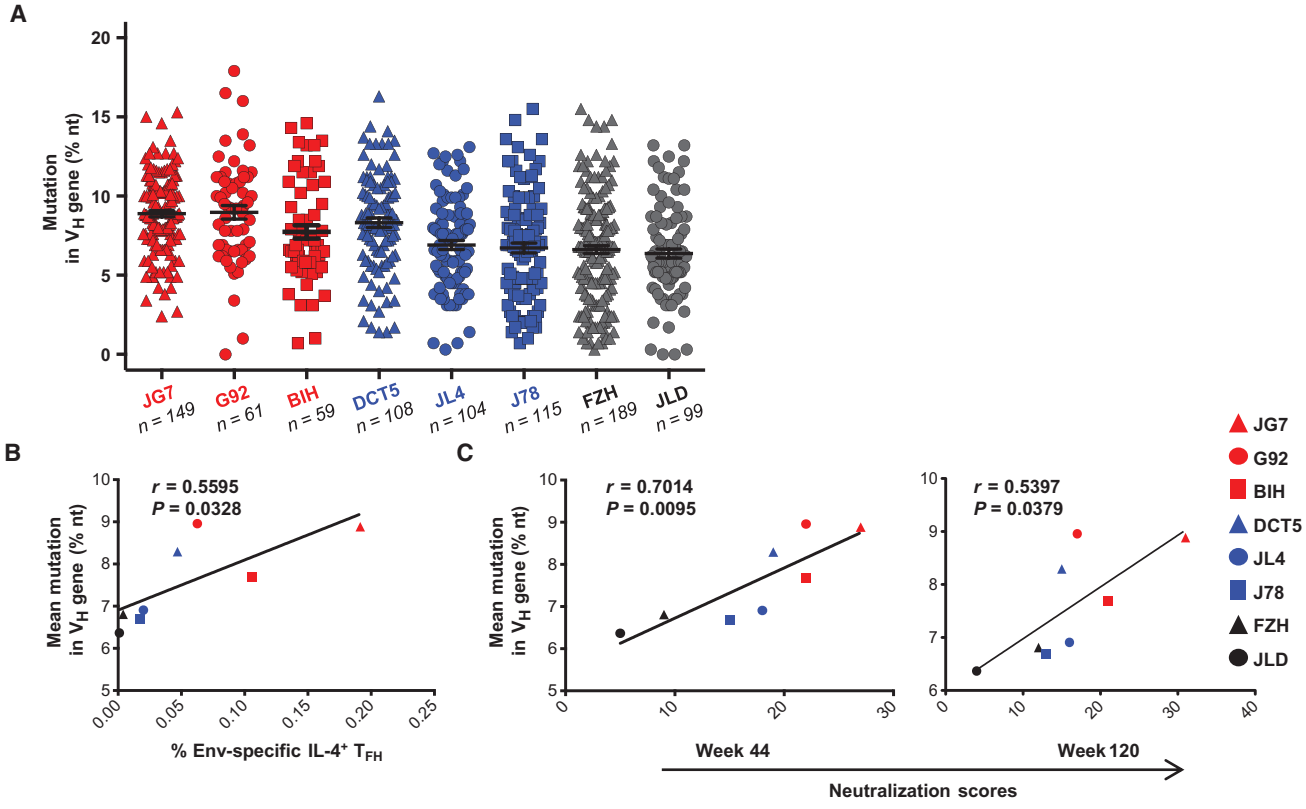

Fig. 4. Expansion of highly mutated clonal families of gp140-specific B cells. (**A**) Percent mutation in the V_H gene for single cell–sorted B cells graphed for each SHIV-infected RM. Each symbol represents a single BCR analyzed, and the number (*n*) of BCRs sequenced per RM is noted in the *x* axis. (**B** and **C**) Mean mutation in the V_H gene per RM is plotted as a function of the percentage of Env-specific IL-4^+ T_{FH} cells (B) and as a function of neutralization scores over time (C). Lines indicate correlations determined by linear regression analysis. nt, nucleotide.

on the virus to neutralize diverse HIV strains. Furthermore, our observations concur with a recent study of an HIV-infected individual, demonstrating that diversification of the T/F virus precedes development of antibody breadth indicating B cell and virus coevolution (*39*). It was recently reported that newly activated T cells can also enter established GCs (*40*), raising the possibility that T cell escape may lead to the generation of T_{FH} cells targeting new epitopes that can then join, and potentially prolong, the GC reaction. Overall, high viral load and *env* gene diversity appear to be the primary determinants of Env-specific T_{FH} and GC B cell accumulation, which then drive the affinity maturation process. It is possible that a strong T_H1 response controls virus in the low neutralizing RMs; however, we found no correlation between frequency of Env-specific IFNγ-producing CD8 cells and virus load.

Multiple memory T_{FH}-like subsets have been identified in the blood that associate with antibody responses to vaccination (*41*, *42*), infection (*35*), and autoimmune disease (*43*), indicating that memory T_{FH}-like cells in the blood could be a surrogate for T_{FH} and GC reactions in secondary lymphoid tissues. Consistent with our previous studies (*44*), we failed to detect a correlation between blood T_{FH}-like subsets or antigen-specific blood T_{FH} cells and neutralization activity

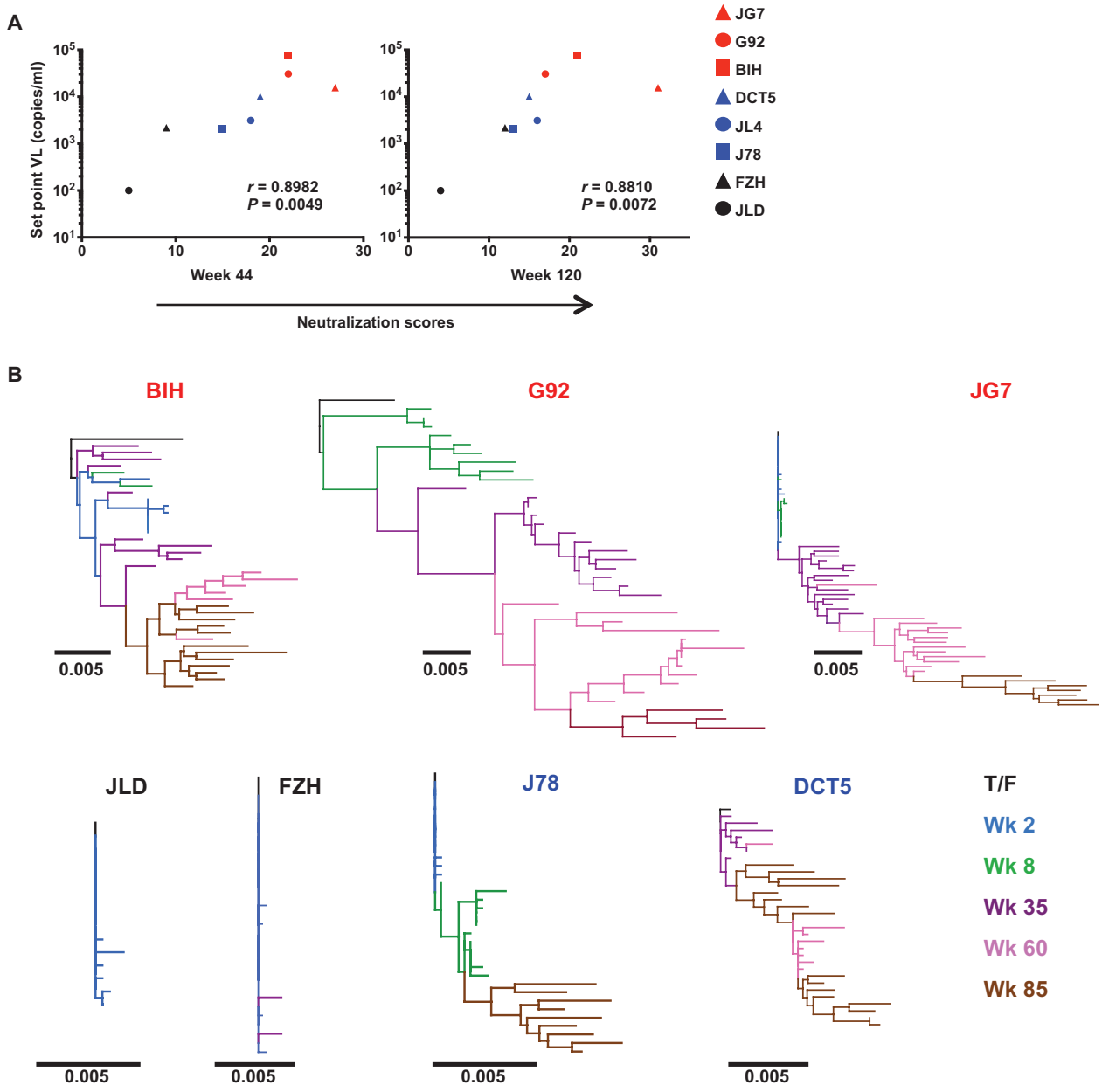

Fig. 5. Viral diversity expansion over time preceding the development of neutralizing activity. (**A**) Mean set point log_{10} viral load (VL) correlates with neutralization score at weeks 44 and 120 PI. (**B**) Maximum likelihood trees of *env* gene sequences display phylogenetic diversity longitudinally during $SHIV_{AD8}$ infection. Sequential sequences from 2 to 80 weeks PI (as indicated) are visualized as phylograms rooted to the transmitted/founder *env* sequence $SHIV_{AD8\text{-}EO}$. No sequences were amplified from JL4.

(fig. S13). Thus, in this model of chronic lentiviral infection, T_{FH}-like memory cells in the blood were not directly indicative of T_{FH}-B cell interactions in the LN.

Our study can help address whether antigen-specific T_{FH} cells generated in a chronic viral infection are beneficial or detrimental to the overall antiviral immune response. In mice, T_{FH} cell expansion helps control chronic lymphocytic choriomeningitis virus infection (*13*). However, T_{FH} cell expansion is not associated with virologic control in HIV/SIV infection. The data suggest that the high levels of continuous Env antigen production are necessary for driving the GC reactions that lead to more effective antibody responses. It is possible that virologic control, whether through T cell, innate, or antibody-mediated mechanisms, could retard the evolution of NAbs.

How can we recapitulate these processes through vaccination? Because generalized immune activation and increased IL-6 production help drive T_{FH} cell differentiation during HIV/SIV/SHIV infection, the selection of appropriate adjuvants for vaccination may be crucial. However, a number of adjuvants have been assessed and demonstrated no impact on SHM levels in Env-specific B cells as compared to unadjuvanted vaccines (*19*). Because persistent production of viral Env glycoproteins appears to be essential to maintain T_{FH} cells in LNs (*10*, *13*, *45*), the use of replication-competent vectors may be required to maintain T_{FH} cells for the length of time necessary to drive B cell affinity maturation. It is unclear if the expression of antigen in and by T_{FH} cells, as seen in chronic HIV/SIV/SHIV infection, will be required of replication-competent vectors, or if cell-free expression will be sufficient. Finally, whether or not chronic antigen persistence, in the absence of sequence evolution, will drive the degree of affinity maturation and SHM required for a strong and broad NAb response remains to be determined.

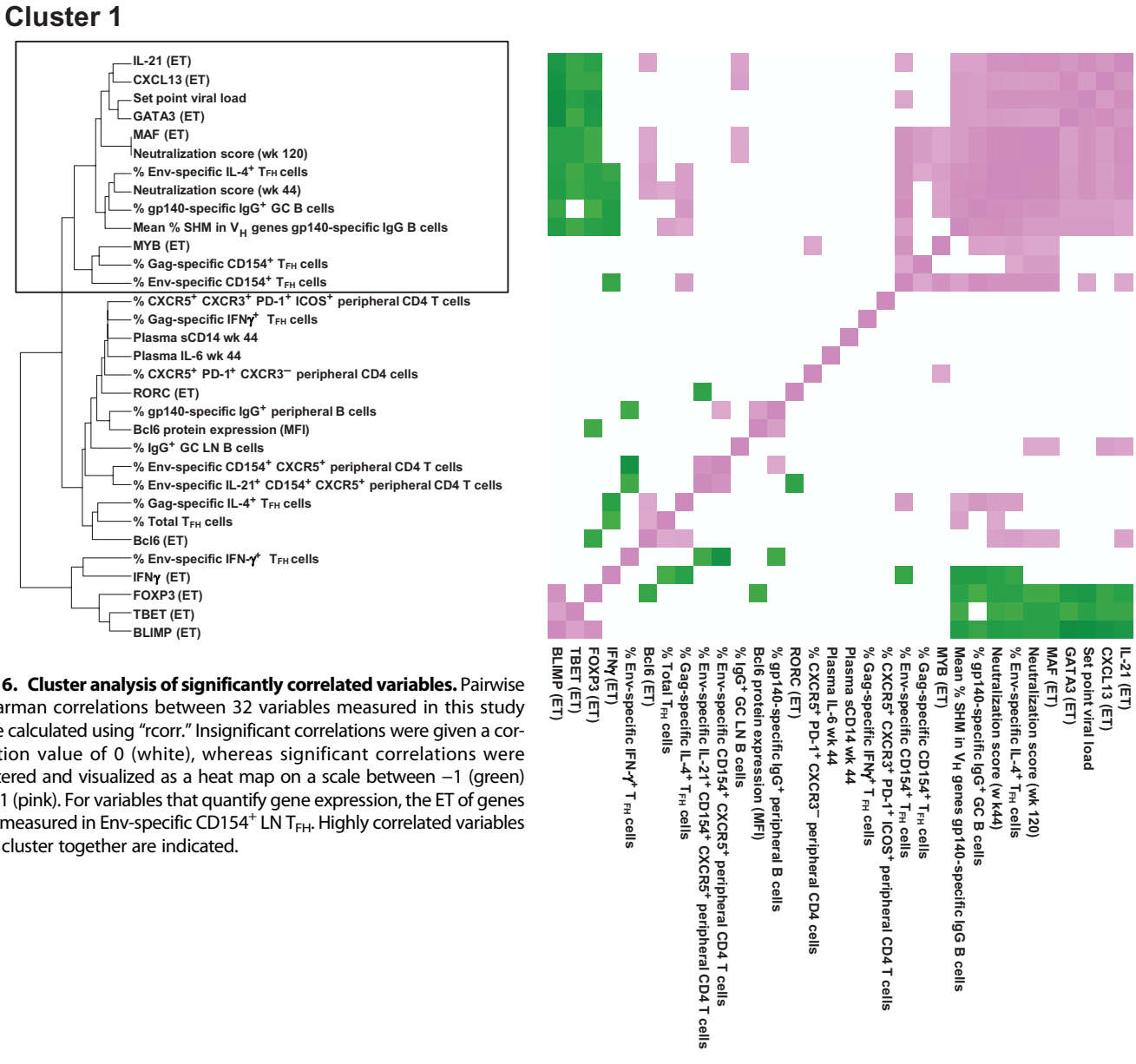

Fig. 6. Cluster analysis of significantly correlated variables. Pairwise Spearman correlations between 32 variables measured in this study were calculated using "rcorr." Insignificant correlations were given a correlation value of 0 (white), whereas significant correlations were clustered and visualized as a heat map on a scale between −1 (green) and 1 (pink). For variables that quantify gene expression, the ET of genes was measured in Env-specific $CD154^+$ LN T_{FH}. Highly correlated variables that cluster together are indicated.

MATERIALS AND METHODS

Study design

The overall objective of this study was to analyze the variables associated with T_{FH} activation and B cell maturation during SHIV infection of RMs as a model for HIV-1 infection. Analysis of both gene and protein expression was performed on defined cell types and functional assays. There was no blinding or randomization of samples.

Virus

The origin and preparation of the tissue culture–derived $SHIV_{AD8}$ swarm and molecular cloned stocks have been previously described (*6*, *7*).

Animal experiments

Eight male and female RMs (*Macaca mulatta*) of Indian genetic origin ranging from 2 to 8 years of age were maintained in accordance with Guide for the Care and Use of Laboratory Animals Report no. NIH 85-23 (Department of Health and Human Services, Bethesda, MD, 1985) and were housed in a biosafety level 2 National Institute of Allergy and Infectious Diseases (NIAID) facility. Phlebotomies and sample collection were performed as previously described (*46*). All animals were negative for the major histocompatibility complex class I *Mamu-A*01*, *Mamu-B*08*, and *Mamu-B*17* alleles.

Quantification of viral nucleic acids

Viral RNA levels in plasma were determined by real-time RT-PCR (ABI PRISM 7900HT sequence detection system; Applied Biosystems) as previously reported (*46*).

Antibodies

We used the following directly conjugated antibodies: CD3-Cy7APC (allophycocyanin) (SP34-2), CD95-Cy5PE (phycoerythrin) (DX-2), CXCR3–Alexa 700, IL-4–Cy7PE (8D4-8), IFNγ-FITC (fluorescein isothiocyanate), CD154-PE (TRAP1), IL-21–Alexa 647 IgG-APC, IgM-V450, and CD4-BV605 (all from BD Biosciences); CD8-BV785, CD20-BV570, CCR7-BV421, PD-1–BV785, ICOS–Pacific Blue, and streptavidin-BV650 (all from BioLegend); CD14–Qdot 800 (Invitrogen); CD28-ECD (CD28.2), CD19-ECD, and CD27-PC5 (Beckman Coulter); CXCR5–PerCP-eFluor 710 and CXCR5-APC (MU5UBEE) (eBioscience); and biotinylated anti–PD-1 (R&D Systems). Aqua amine viability dye was purchased from Invitrogen; IgD-FITC was obtained from Southern-Biotech; streptavidin-Cy7PE was obtained from Molecular Probes; and peanut agglutinin (PNA)–PE was purchased from GeneTex. To detect antigen-specific B cells, an uncleaved, stable trimerized gp140 YU2 protein was used (*47*). The Avi-tagged YU2 gp140 protein was expressed, purified, and biotinylated using the biotin ligase BirA (Avidity) (*48*). Biotinylation of the YU2 gp140 protein was confirmed by enzyme-linked immunosorbent assay (ELISA). The protein was then conjugated with the streptavidin-fluorochrome reagents, streptavidin-Cy7PE (Invitrogen).

Polychromatic flow cytometry

To detect antigen-specific T_{FH} cells, we performed surface and intracellular cytokine staining of $CD4^+$ T cells. Briefly, 4×10^6 to 5×10^6 LN cells were incubated in 1 ml of medium containing monensin (0.7 μg/ml; BD Biosciences) and brefeldin A (10 μg/ml; Sigma-Aldrich) in the absence or presence of peptides (15-mers overlapping by 11 residues) corresponding to full-length SIV Gag or HIV clade B Env [2 μg/ml each peptide, 5 μl/ml; National Institutes of Health (NIH) AIDS Reagent Program] for 8 hours. After washing, cells were stained with Aqua and anti–PD-1 biotin. Following a staining step with streptavidin, cells were surface-stained with titrated amounts of αCD4, αCD8, αCD20, αCD14, αCD28, αCD95, αCXCR5, and αCCR7. After fix/permeabilization, cells were stained with αCD3, αCD154, αIL-4, αIL-21, and αIFNγ. Aqua was used to exclude dead cells from the analysis. Between 2×10^6 and 3×10^6 events were collected in each case. Electronic compensation was conducted with antibody capture beads (BD Biosciences) stained separately with individual mAbs used in the test samples. Data were analyzed using FlowJo version 9.7 (Tree Star). Forward scatter area versus forward scatter height was used to gate out cell aggregates. $CD14^+$, $CD20^+$, and dead cells were removed from the analysis to reduce background staining. To detect antigen-specific B cells, 2×10^6 to 3×10^6 PBMCs, LN cells, and BM cells were stained with Aqua and biotinylated YU2 gp140 probe on ice for 30 min. Following a staining step with streptavidin, cells were surface-stained with titrated amounts of αCD3, αCD8, αCD20, αCD14, αCD27, αIgD, αIgM, αIgG, and PNA. Forward scatter area versus forward scatter height was used to gate out cell aggregates. $CD14^+$, $CD3^+$, $CD8^+$, and dead cells were removed from the analysis to reduce background staining. To detect transcription factors, we performed surface and intracellular transcription factor staining of $CD4^+$ T cells. Briefly, 4×10^6 to 5×10^6 LN cells were stained with αCD4, αCD8, αCD20, αCD14, αCD28, αCD95, αCXCR5, and αCCR7. After fix/permeabilization by Transcription Factor Buffer (BD Biosciences), cells were stained with αBcl6 (clone K112-91 from BD Biosciences), αGATA3 (clone L50-823 from BD Biosciences), αT-bet (clone 4B10 from BioLegend), and/or aRORγt (clone Q21-559 from BD Biosciences).

Quantitative reverse transcription polymerase chain reaction

mRNA was purified from sorted $CD154^+$ T_{FH} cells and analyzed using the SuperScript III Platinum One-Step qRT-PCR system (Invitrogen). For ease of data interpretation, "ET" values are reported throughout the article; these values are equal to $40 - C_t$ and thus increase with greater expression of a transcript; they are proportional to $\log_2$ RNA abundance. The two-way hierarchical clustering analysis was performed using JMP version 10. The following primers and probes were used: *Bcl6* (Hs00277037_m1), *IL-21* (Hs00222327_m1), *c-MAF* (Hs00193519_m1), *GAPDH* (glyceraldehyde phosphate dehydrogenase) (Hs99999905_m1), *TBX21* (*T-bet*) (Rh02621772_m1), *CXCL13* (Hs00757930_m1), *GATA3* (Rh02830714_m1), *MYB* (Hs00920554_m1), *Foxp3* (Rh02788830_m1), *IFNγ* (Rh02788577_m1), *PRDM1* (*Blimp1*) (Rh02837836_m1), and *RORC* (Rh02892670_m1).

Measurement of sCD14 and IL-6 levels

sCD14 and IL-6 levels were determined in plasma by ELISA according to the manufacturer's instructions (R&D Systems, catalog no. DC140 for sCD14 and catalog no. D6050 for IL-6).

Neutralization assays

Plasma neutralizing activity against pseudotyped HIV-1 isolates and SHIVs was measured using the TZM-bl luciferase reporter gene assay as described (*49*, *50*). Pseudoviruses were diluted to obtain a baseline infection level of ~200,000 relative light units. Neutralization curves were fit using a five-parameter hill-slope equation (*50*). Reciprocal dilutions required to inhibit infection by 50% are reported as ID_{50}s.

Sequence analysis of the heavy chain variable region of Env-specific B cells

Antigen-specific B cells were single cell–sorted as previously described (*51*, *52*). Briefly, BM B cells with the phenotype of $IgD^{-}IgM^{-}CD27^{+}IgG^{+}$YU2-$gp140^{+}$ were single cell–sorted into 96-well PCR plates containing 20 μl of lysis buffer per well. The lysis buffer contained 0.5 μl of RNaseOUT (Invitrogen), 5 μl of 5× First-Strand Buffer (Invitrogen), 1.25 μl of 0.1 M dithiothreitol (DTT) (Invitrogen), and 0.0625 μl of Igepal (Sigma). RT was carried out by adding 3 μl of random hexamers (Gene Link) at 150 ng/μl, 2 μl of deoxynucleoxide triphosphate (dNTP) mix, each at 10 mM, and 1 μl of SuperScript III (Invitrogen) into each well for 42°C for 10 min, 25°C for 10 min, 50°C for 60 min, and 94°C for 5 min. The IgH variable region genes were amplified independently by nested PCR starting from 4 μl of complementary DNA (cDNA) as template. All PCRs were performed in 96-well PCR plates in a total volume of 25 μl containing water, 2.5 μl of 10× buffer, 0.5 μl of dNTP mix, each at 10 mM, 5 μl Q-Solution (Qiagen), 0.4 μl of HotStarTaq *Plus* DNA Polymerase (Qiagen), and 0.5 μl of primer or primer mix for each direction at 25 μM. For the first-round PCR 0.25 μl of $MgCl_2$ at 25 mM (Qiagen), Forward L1 primer mix, and Reverse 3′IgG(Outer) were used, whereas for the second-round PCR, the Forward SE primer mix and Reverse 3′IgG(Inner) were used as described before (*51*). Each round of PCR was initiated at 94°C for 5 min, followed by 50 cycles of 94°C for 30 s, 55°C for the first round or 60°C for the second round for 30 s, and 70°C for 1 min, followed by 70°C for 10 min. The positive second-round PCR products were direct-sequenced with reverse PCR primers. Sequences containing stop codons, frameshifts, ambiguous nucleotide calls, or alignment lengths less than 250 nucleotides were not considered. Reads were further filtered for length, keeping only those between 300 and 600 nucleotides. Germline V genes were then assigned to each read using BLAST (Basic Local Alignment Search Tool) with empirically optimized parameters (*53*). Reads for which no V gene match was found with an *e* value $\leq 10^{-10}$ were discarded. ClustalW2 was used to calculate the sequence identity to the germ line of each BCR using a newly described RM database (*19*, *54*). BCR sequences were deposited in GenBank with accession nos. KM097097 to KM097988.

Cloning of highly mutated Env-specific B cells

First-round PCR products for single cell–sorted YU2 gp140f-specific B cells were reamplified with custom primers containing restriction digest sites followed by subcloning, expression, and purification as described before (*52*). Heavy chains were reconstituted as IgG1. The full-length IgG1 was expressed by cotransfection of 293 F cells with equal amounts of the paired heavy and light chain plasmids and purified using a recombinant protein A column (GE Healthcare). The antibody names are designated with a "donor-antibody lineage.clone" convention. Sequences of cloned heavy and light chain mAbs JG7-VRC30.01-VRC32.01 were deposited in GenBank with accession nos. KM103065 to KM103076.

Viral RNA extraction and cDNA synthesis

From each plasma specimen, at least 20,000 viral RNA copies were extracted using the QIAamp Viral RNA Mini kit (Qiagen). RT of RNA to single-stranded cDNA was performed using SuperScript III Reverse Transcriptase according to the manufacturer's recommendations (Invitrogen). In brief, a cDNA reaction of 1× RT buffer, 0.5 mM of each dNTP, 5 mM DTT, RNaseOUT [RNase (recombinant ribonuclease) inhibitor] (2 U/ml),SuperScript III Reverse Transcriptase (10 U/ml), and 0.25 mM antisense primer SIVEnvR1 5′-TGTAATAAATCCCTTCCAGTCCCCCC-3′ was incubated at 50°C for 60 min and 55°C for 60 min and then heat-inactivated at 70°C for 15 min followed by treatment with 2 U of RNase H at 37°C for 20 min. The newly synthesized cDNA was used immediately or frozen at −80°C.

Single-genome amplification of SHIV *env*

A 3.3-kb fragment that includes the entire *env* gene was sequenced from each animal at various time points after infection using a limiting dilution PCR so that only one amplifiable molecule is present in each reaction. Single-genome amplification was performed by serially diluting cDNA distributed among independent PCRs to identify a dilution where amplification occurred in <30% of the total number of reactions. PCR amplification was performed with 1× PCR buffer, 2 mM $MgSO_4$, 0.2 mM of each dNTP, 0.2 μM of each primer, and Platinum Taq High Fidelity polymerase (0.025 U/μl) (Invitrogen) in a 20-μl reaction. First-round PCR was performed with primer SIVEnvF1 5′-CCTCCCCCTCCAGGACTAGC-3′ and antisense primer SIVEnvR1 under the following conditions: 1 cycle of 94°C for 2 min and 35 cycles at 94°C for 15 s, 55°C for 30 s, and 68°C for 5 min, followed by a final extension of 68°C for 10 min. Next, 1 μl from the first-round PCR product was added to a second-round PCR that included the sense primer SHIVEnvF2 5′-GACCTCCAGAAAATGAAGGACCAC-3′ and antisense primer SIVEnvR2 5′-ATGAGACATRTCTATTGCCAATTTGTA-3′ performed under the same conditions used for first-round PCR, but with a total of 45 cycles. Correct sized amplicons were identified by agarose gel electrophoresis and directly sequenced with second-round PCR primers and nine HIV-specific primers using BigDye Terminator technology (Applied Biosystems). To confirm PCR amplification from a single template, chromatograms were manually examined for multiple peaks, indicative of the presence of amplicons resulting from PCR-generated recombination events, *Taq* polymerase errors, or multiple variant templates.

Sequence alignments, diversity, and phylogenetic analysis

Sequences were codon-aligned to the infecting transmitted founder (T/F) clone $SHIV_{AD8\text{-}EO\text{-}RQ}$ and manually edited using Geneious version 6 (Biomatters; www.geneious.com/). The *env* sequences containing unproductive mutations (such as those that cause stop codons and frameshifts) were removed from further analysis. Maximum likelihood trees were constructed using RaxML on the CIPRES Science Gateway (1) and visualized as rooted to the T/F using the FigTree program. All sequences were deposited in GenBank with accession nos. KM082157 to KM082524.

Enzyme-linked immunosorbent assay

ELISAs were performed as previously described (*52*). Briefly, 96-well ELISA plates were coated with the specified recombinant protein (2 μg/ml) in phosphate-buffered saline (PBS) overnight at 4°C. The following day, the plates were blocked with B3T buffer (150 mM NaCl, 50 mM tris-HCl, 1 mM EDTA, 3.3% fetal bovine serum, 2% bovine albumin, and 0.07% Tween 20) and incubated with fourfold serial dilutions of heat-inactivated plasma starting at a dilution of 1:100 followed by peroxidase-conjugated goat anti-human IgG antibody (Jackson ImmunoResearch). All incubations were for 1 hour at 37°C, and all volumes were 100 μl except that for blocking, which was 200 μl. Plates were washed between each incubation with 0.1% Tween 20 in PBS, detected using SureBlue TMB (3,3′,5,5′-tetramethylbenzidine) substrate (Kirkegaard & Perry Laboratories), and subsequently read at 450 nm. For competition ELISA, plates were coated with sheep anti-gp120 C5 antibody (1 μg/ml) (Aalto Bio Reagents) overnight and then used to capture YU2 gp120 protein. After blocking,

serial dilutions of competition antibodies were added for gp120 binding followed by biotin-labeled JG7-VRC30.02 (150 ng/ml) for 1 hour. Plates were next incubated with streptavidin–horseradish peroxidase (250 ng/ml) (Sigma) and developed with TMB as described above.

Statistical analysis

Statistical methods used here comply with journal guidelines. Experimental variables were analyzed using the Wilcoxon matched-pairs signed rank test with normal-based 95% confidence interval; correlations were performed using the nonparametric Spearman rank test and linear regression analysis. Bars depict median values, and P values of <0.05 were considered significant. The GraphPad Prism statistical analysis program (GraphPad Software) was used throughout. For analysis of all 32 variables measured during infection, pairwise correlations with significance levels were calculated using rcorr from the R package "Hmisc." When a pairwise correlation was determined to be significant, the correlation value was retained. When a correlation was determined to be insignificant, the correlation value was set to zero. The remaining significant correlations were then clustered and visualized as a heat map using the R package "heatmap.2."

SUPPLEMENTARY MATERIALS

www.sciencetranslationalmedicine.org/cgi/content/full/7/298/298ra120/DC1
Fig. S1. Gating scheme for T_{FH}.
Fig. S2. Plasma sCD14 levels and IL-6 levels of RMs.
Fig. S3. Longitudinal development of NAbs during $SHIV_{AD8}$ infection.
Fig. S4. Representative gating scheme used for the quantification of Env-specific B cells in an LN.
Fig. S5. Total T_{FH} and IgG^+ B cells.
Fig. S6. Quantification of HIV Gag and Env-specific T_{FH} cells.
Fig. S7. Antigen-specific responses in the LN.
Fig. S8. Gating scheme for Bcl6 expression in T_{FH} cells.
Fig. S9. Gene signatures of Env-specific $CD154^+$ T_{FH} cells.
Fig. S10. Expansion of highly mutated clonal families of gp140-specific B cells.
Fig. S11. Neutralization by affinity-matured antibodies.
Fig. S12. Epitope mapping of JG7-VRC30 family of mAbs.
Fig. S13. The frequency of peripheral T_{FH} (pT_{FH})–like cells does not predict broad neutralization activity.
Table S1. Source data.

REFERENCES AND NOTES

1. P. D. Kwong, J. R. Mascola, G. J. Nabel, Broadly neutralizing antibodies and the search for an HIV-1 vaccine: The end of the beginning. *Nat. Rev. Immunol.* **13**, 693–701 (2013).
2. S. Crotty, Follicular helper CD4 T cells (T_{FH}). *Annu. Rev. Immunol.* **29**, 621–663 (2011).
3. C. Petrovas, T. Yamamoto, M. Y. Gerner, K. L. Boswell, K. Wloka, E. C. Smith, D. R. Ambrozak, N. G. Sandler, K. J. Timmer, X. Sun, L. Pan, A. Poholek, S. S. Rao, J. M. Brenchley, S. M. Alam, G. D. Tomaras, M. Roederer, D. C. Douek, R. A. Seder, R. N. Germain, E. K. Haddad, R. A. Koup, CD4 T follicular helper cell dynamics during SIV infection. *J. Clin. Invest.* **122**, 3281–3294 (2012).
4. N. Fazilleau, L. Mark, L. J. McHeyzer-Williams, M. G. McHeyzer-Williams, Follicular helper T cells: Lineage and location. *Immunity* **30**, 324–335 (2009).
5. M. McHeyzer-Williams, S. Okitsu, N. Wang, L. McHeyzer-Williams, Molecular programming of B cell memory. *Nat. Rev. Immunol.* **12**, 24–34 (2012).
6. R. Gautam, Y. Nishimura, W. R. Lee, O. Donau, A. Buckler-White, M. Shingai, R. Sadjadpour, S. D. Schmidt, C. C. LaBranche, B. F. Keele, D. Montefiori, J. R. Mascola, M. A. Martin, Pathogenicity and mucosal transmissibility of the R5-tropic simian/human immunodeficiency virus $SHIV_{AD8}$ in rhesus macaques: Implications for use in vaccine studies. *J. Virol.* **86**, 8516–8526 (2012).
7. M. Shingai, O. K. Donau, S. D. Schmidt, R. Gautam, R. J. Plishka, A. Buckler-White, R. Sadjadpour, W. R. Lee, C. C. LaBranche, D. C. Montefiori, J. R. Mascola, Y. Nishimura, M. A. Martin, Most rhesus macaques infected with the CCR5-tropic $SHIV_{AD8}$ generate cross-reactive antibodies that neutralize multiple HIV-1 strains. *Proc. Natl. Acad. Sci. U.S.A.* **109**, 19769–19774 (2012).
8. L. M. Walker, D. Sok, Y. Nishimura, O. Donau, R. Sadjadpour, R. Gautam, M. Shingai, R. Pejchal, A. Ramos, M. D. Simek, Y. Geng, I. A. Wilson, P. Poignard, M. A. Martin, D. R. Burton, Rapid development of glycan-specific, broad, and potent anti–HIV-1 gp120 neutralizing antibodies in an R5 SIV/HIV chimeric virus infected macaque. *Proc. Natl. Acad. Sci. U.S.A.* **108**, 20125–20129 (2011).
9. I. S. Georgiev, N. A. Doria-Rose, T. Zhou, Y. D. Kwon, R. P. Staupe, S. Moquin, G. Y. Chuang, M. K. Louder, S. D. Schmidt, H. R. Altae-Tran, R. T. Bailer, K. McKee, M. Nason, S. O'Dell, G. Ofek, M. Pancera, S. Srivatsan, L. Shapiro, M. Connors, S. A. Migueles, L. Morris, Y. Nishimura, M. A. Martin, J. R. Mascola, P. D. Kwong, Delineating antibody recognition in polyclonal sera from patterns of HIV-1 isolate neutralization. *Science* **340**, 751–756 (2013).
10. M. Lindqvist, J. van Lunzen, D. Z. Soghoian, B. D. Kuhl, S. Ranasinghe, G. Kranias, M. D. Flanders, S. Cutler, N. Yudanin, M. I. Muller, I. Davis, D. Farber, P. Hartjen, F. Haag, G. Alter, J. Schulze zur Wiesch, H. Streeck, Expansion of HIV-specific T follicular helper cells in chronic HIV infection. *J. Clin. Invest.* **122**, 3271–3280 (2012).
11. M. Perreau, A. L. Savoye, E. De Crignis, J. M. Corpataux, R. Cubas, E. K. Haddad, L. De Leval, C. Graziosi, G. Pantaleo, Follicular helper T cells serve as the major CD4 T cell compartment for HIV-1 infection, replication, and production. *J. Exp. Med.* **210**, 143–156 (2013).
12. N. G. Sandler, H. Wand, A. Roque, M. Law, M. C. Nason, D. E. Nixon, C. Pedersen, K. Ruxrungtham, S. R. Lewin, S. Emery, J. D. Neaton, J. M. Brenchley, S. G. Deeks, I. Sereti, D. C. Douek; INSIGHT SMART Study Group, Plasma levels of soluble CD14 independently predict mortality in HIV infection. *J. Infect. Dis.* **203**, 780–790 (2011).
13. J. A. Harker, G. M. Lewis, L. Mack, E. I. Zuniga, Late interleukin-6 escalates T follicular helper cell responses and controls a chronic viral infection. *Science* **334**, 825–829 (2011).
14. R. I. Nurieva, Y. Chung, D. Hwang, X. O. Yang, H. S. Kang, L. Ma, Y. H. Wang, S. S. Watowich, A. M. Jetten, Q. Tian, C. Dong, Generation of T follicular helper cells is mediated by interleukin-21 but independent of T helper 1, 2, or 17 cell lineages. *Immunity* **29**, 138–149 (2008).
15. C. H. Kim, H. W. Lim, J. R. Kim, L. Rott, P. Hillsamer, E. C. Butcher, Unique gene expression program of human germinal center T helper cells. *Blood* **104**, 1952–1960 (2004).
16. R. L. Reinhardt, H. E. Liang, R. M. Locksley, Cytokine-secreting follicular T cells shape the antibody repertoire. *Nat. Immunol.* **10**, 385–393 (2009).
17. M. A. Linterman, L. Beaton, D. Yu, R. R. Ramiscal, M. Srivastava, J. J. Hogan, N. K. Verma, M. J. Smyth, R. J. Rigby, C. G. Vinuesa, IL-21 acts directly on B cells to regulate Bcl-6 expression and germinal center responses. *J. Exp. Med.* **207**, 353–363 (2010).
18. G. D. Victora, M. C. Nussenzweig, Germinal centers. *Annu. Rev. Immunol.* **30**, 429–457 (2012).
19. J. R. Francica, Z. Sheng, Z. Zhang, Y. Nishimura, M. Shingai, A. Ramesh, B. F. Keele, S. D. Schmidt, B. J. Flynn, S. Darko, R. M. Lynch, T. Yamamoto, R. Matus-Nicodemos, D. Wolinsky; NISC Comparative Sequencing Program, M. Nason, N. M. Valiante, P. Malyala, E. De Gregorio, S. W. Barnett, M. Singh, D. T. O'Hagan, R. A. Koup, J. R. Mascola, M. A. Martin, T. B. Kepler, D. C. Douek, L. Shapiro, R. A. Seder, Analysis of immunoglobulin transcripts and hypermutation following $SHIV_{AD8}$ infection and protein-plus-adjuvant immunization. *Nat. Commun.* **6**, 6565 (2015).
20. C. Sundling, Z. Zhang, G. E. Phad, Z. Sheng, Y. Wang, J. R. Mascola, Y. Li, R. T. Wyatt, L. Shapiro, G. B. Karlsson Hedestam, Single-cell and deep sequencing of IgG-switched macaque B cells reveal a diverse Ig repertoire following immunization. *J. Immunol.* **192**, 3637–3644 (2014).
21. M. P. Lefranc, V. Giudicelli, C. Ginestoux, J. Jabado-Michaloud, G. Folch, F. Bellahcene, Y. Wu, E. Gemrot, X. Brochet, J. Lane, L. Regnier, F. Ehrenmann, G. Lefranc, P. Duroux, $IMGT^®$, the international ImMunoGeneTics information system. *Nucleic Acids Res.* **37**, D1006–D1012 (2009).
22. C. C. Huang, M. Venturi, S. Majeed, M. J. Moore, S. Phogat, M. Y. Zhang, D. S. Dimitrov, W. A. Hendrickson, J. Robinson, J. Sodroski, R. Wyatt, H. Choe, M. Farzan, P. D. Kwong, Structural basis of tyrosine sulfation and V_H-gene usage in antibodies that recognize the HIV type 1 coreceptor-binding site on gp120. *Proc. Natl. Acad. Sci. U.S.A.* **101**, 2706–2711 (2004).
23. N. A. Doria-Rose, R. M. Klein, M. G. Daniels, S. O'Dell, M. Nason, A. Lapedes, T. Bhattacharya, S. A. Migueles, R. T. Wyatt, B. T. Korber, J. R. Mascola, M. Connors, Breadth of human immunodeficiency virus-specific neutralizing activity in sera: Clustering analysis and association with clinical variables. *J. Virol.* **84**, 1631–1636 (2010).
24. I. Mikell, D. N. Sather, S. A. Kalams, M. Altfeld, G. Alter, L. Stamatatos, Characteristics of the earliest cross-neutralizing antibody response to HIV-1. *PLOS Pathog.* **7**, e1001251 (2011).
25. A. Piantadosi, D. Panteleeff, C. A. Blish, J. M. Baeten, W. Jaoko, R. S. McClelland, J. Overbaugh, Breadth of neutralizing antibody response to human immunodeficiency virus type 1 is affected by factors early in infection but does not influence disease progression. *J. Virol.* **83**, 10269–10274 (2009).
26. R. A. Cubas, J. C. Mudd, A. L. Savoye, M. Perreau, J. van Grevenynghe, T. Metcalf, E. Connick, A. Meditz, G. J. Freeman, G. Abesada-Terk Jr., J. M. Jacobson, A. D. Brooks, S. Crotty, J. D. Estes, G. Pantaleo, M. M. Lederman, E. K. Haddad, Inadequate T follicular cell help impairs B cell immunity during HIV infection. *Nat. Med.* **19**, 494–499 (2013).
27. L. Stamatatos, L. Morris, D. R. Burton, J. R. Mascola, Neutralizing antibodies generated during natural HIV-1 infection: Good news for an HIV-1 vaccine? *Nat. Med.* **15**, 866–870 (2009).
28. S. Moir, A. S. Fauci, B cells in HIV infection and disease. *Nat. Rev. Immunol.* **9**, 235–245 (2009).
29. P. Hraber, M. S. Seaman, R. T. Bailer, J. R. Mascola, D. C. Montefiori, B. T. Korber, Prevalence of broadly neutralizing antibody responses during chronic HIV-1 infection. *AIDS* **28**, 163–169 (2014).

30. A. D. Gitlin, Z. Shulman, M. C. Nussenzweig, Clonal selection in the germinal centre by regulated proliferation and hypermutation. *Nature* **509**, 637–640 (2014).
31. R. R. Ramiscal, C. G. Vinuesa, T-cell subsets in the germinal center. *Immunol. Rev.* **252**, 146–155 (2013).
32. D. Baumjohann, S. Preite, A. Reboldi, F. Ronchi, K. M. Ansel, A. Lanzavecchia, F. Sallusto, Persistent antigen and germinal center B cells sustain T follicular helper cell responses and phenotype. *Immunity* **38**, 596–605 (2013).
33. R. I. Nurieva, Y. Chung, G. J. Martinez, X. O. Yang, S. Tanaka, T. D. Matskevitch, Y. H. Wang, C. Dong, Bcl6 mediates the development of T follicular helper cells. *Science* **325**, 1001–1005 (2009).
34. D. Yu, S. Rao, L. M. Tsai, S. K. Lee, Y. He, E. L. Sutcliffe, M. Srivastava, M. Linterman, L. Zheng, N. Simpson, J. I. Ellyard, I. A. Parish, C. S. Ma, Q. J. Li, C. R. Parish, C. R. Mackay, C. G. Vinuesa, The transcriptional repressor Bcl-6 directs T follicular helper cell lineage commitment. *Immunity* **31**, 457–468 (2009).
35. M. Locci, C. Havenar-Daughton, E. Landais, J. Wu, M. A. Kroenke, C. L. Arlehamn, L. F. Su, R. Cubas, M. M. Davis, A. Sette, E. K. Haddad; International AIDS Vaccine Initiative Protocol C Principal Investigators, P. Poignard, S. Crotty, Human circulating PD-1^{+}CXCR3^{-}CXCR5^{+} memory Tfh cells are highly functional and correlate with broadly neutralizing HIV antibody responses. *Immunity* **39**, 758–769 (2013).
36. D. N. Sather, J. Armann, L. K. Ching, A. Mavrantoni, G. Sellhorn, Z. Caldwell, X. Yu, B. Wood, S. Self, S. Kalams, L. Stamatatos, Factors associated with the development of cross-reactive neutralizing antibodies during human immunodeficiency virus type 1 infection. *J. Virol.* **83**, 757–769 (2009).
37. J. R. Mascola, B. F. Haynes, HIV-1 neutralizing antibodies: Understanding nature's pathways. *Immunol. Rev.* **254**, 225–244 (2013).
38. C. G. Vinuesa, S. G. Tangye, B. Moser, C. R. Mackay, Follicular B helper T cells in antibody responses and autoimmunity. *Nat. Rev. Immunol.* **5**, 853–865 (2005).
39. H. X. Liao, R. Lynch, T. Zhou, F. Gao, S. M. Alam, S. D. Boyd, A. Z. Fire, K. M. Roskin, C. A. Schramm, Z. Zhang, J. Zhu, L. Shapiro; NISC Comparative Sequencing Program, J. C. Mullikin, S. Gnanakaran, P. Hraber, K. Wiehe, G. Kelsoe, G. Yang, S. M. Xia, D. C. Montefiori, R. Parks, K. E. Lloyd, R. M. Scearce, K. A. Soderberg, M. Cohen, G. Kamanga, M. K. Louder, L. M. Tran, Y. Chen, F. Cai, S. Chen, S. Moquin, X. Du, M. G. Joyce, S. Srivatsan, B. Zhang, A. Zheng, G. M. Shaw, B. H. Hahn, T. B. Kepler, B. T. Korber, P. D. Kwong, J. R. Mascola, B. F. Haynes, Co-evolution of a broadly neutralizing HIV-1 antibody and founder virus. *Nature* **496**, 469–476 (2013).
40. Z. Shulman, A. D. Gitlin, S. Targ, M. Jankovic, G. Pasqual, M. C. Nussenzweig, G. D. Victora, T follicular helper cell dynamics in germinal centers. *Science* **341**, 673–677 (2013).
41. S. E. Bentebibel, S. Lopez, G. Obermoser, N. Schmitt, C. Mueller, C. Harrod, E. Flano, A. Mejias, R. A. Albrecht, D. Blankenship, H. Xu, V. Pascual, J. Banchereau, A. Garcia-Sastre, A. K. Palucka, O. Ramilo, H. Ueno, Induction of ICOS^{+}CXCR3^{+}CXCR5^{+} T_H cells correlates with antibody responses to influenza vaccination. *Sci. Transl. Med.* **5**, 176ra32 (2013).
42. F. Spensieri, E. Borgogni, L. Zedda, M. Bardelli, F. Buricchi, G. Volpini, E. Fragapane, S. Tavarini, O. Finco, R. Rappuoli, G. Del Giudice, G. Galli, F. Castellino, Human circulating influenza-CD4^{+} ICOS1^{+}IL-21^{+} T cells expand after vaccination, exert helper function, and predict antibody responses. *Proc. Natl. Acad. Sci. U.S.A.* **110**, 14330–14335 (2013).
43. J. He, L. M. Tsai, Y. A. Leong, X. Hu, C. S. Ma, N. Chevalier, X. Sun, K. Vandenberg, S. Rockman, Y. Ding, L. Zhu, W. Wei, C. Wang, A. Karnowski, G. T. Belz, J. R. Ghali, M. C. Cook, D. S. Riminton, A. Veillette, P. L. Schwartzberg, F. Mackay, R. Brink, S. G. Tangye, C. G. Vinuesa, C. R. Mackay, Z. Li, D. Yu, Circulating precursor CCR7^{lo}PD-1^{hi} CXCR5^{+} CD4^{+} T cells indicate Tfh cell activity and promote antibody responses upon antigen reexposure. *Immunity* **39**, 770–781 (2013).
44. K. L. Boswell, R. Paris, E. Boritz, D. Ambrozak, T. Yamamoto, S. Darko, K. Wloka, A. Wheatley, S. Narpala, A. McDermott, M. Roederer, R. Haubrich, M. Connors, J. Ake, D. C. Douek, J. Kim, C. Petrovas, R. A. Koup, Loss of circulating CD4 T cells with B cell helper function during chronic HIV infection. *PLOS Pathog.* **10**, e1003853 (2014).
45. L. M. Fahey, E. B. Wilson, H. Elsaesser, C. D. Fistonich, D. B. McGavern, D. G. Brooks, Viral persistence redirects CD4 T cell differentiation toward T follicular helper cells. *J. Exp. Med.* **208**, 987–999 (2011).
46. Y. Endo, T. Igarashi, Y. Nishimura, C. Buckler, A. Buckler-White, R. Plishka, D. S. Dimitrov, M. A. Martin, Short- and long-term clinical outcomes in rhesus monkeys inoculated with a highly pathogenic chimeric simian/human immunodeficiency virus. *J. Virol.* **74**, 6935–6945 (2000).
47. X. Yang, M. Farzan, R. Wyatt, J. Sodroski, Characterization of stable, soluble trimers containing complete ectodomains of human immunodeficiency virus type 1 envelope glycoproteins. *J. Virol.* **74**, 5716–5725 (2000).
48. J. F. Scheid, H. Mouquet, N. Feldhahn, B. D. Walker, F. Pereyra, E. Cutrell, M. S. Seaman, J. R. Mascola, R. T. Wyatt, H. Wardemann, M. C. Nussenzweig, A method for identification of HIV gp140 binding memory B cells in human blood. *J. Immunol. Methods* **343**, 65–67 (2009).
49. M. Li, F. Gao, J. R. Mascola, L. Stamatatos, V. R. Polonis, M. Koutsoukos, G. Voss, P. Goepfert, P. Gilbert, K. M. Greene, M. Bilska, D. L. Kothe, J. F. Salazar-Gonzalez, X. Wei, J. M. Decker, B. H. Hahn, D. C. Montefiori, Human immunodeficiency virus type 1 *env* clones from acute and early subtype B infections for standardized assessments of vaccine-elicited neutralizing antibodies. *J. Virol.* **79**, 10108–10125 (2005).
50. M. S. Seaman, H. Janes, N. Hawkins, L. E. Grandpre, C. Devoy, A. Giri, R. T. Coffey, L. Harris, B. Wood, M. G. Daniels, T. Bhattacharya, A. Lapedes, V. R. Polonis, F. E. McCutchan, P. B. Gilbert, S. G. Self, B. T. Korber, D. C. Montefiori, J. R. Mascola, Tiered categorization of a diverse panel of HIV-1 Env pseudoviruses for assessment of neutralizing antibodies. *J. Virol.* **84**, 1439–1452 (2010).
51. C. Sundling, G. Phad, I. Douagi, M. Navis, G. B. Karlsson Hedestam, Isolation of antibody V(D)J sequences from single cell sorted rhesus macaque B cells. *J. Immunol. Methods* **386**, 85–93 (2012).
52. X. Wu, T. Zhou, J. Zhu, B. Zhang, I. Georgiev, C. Wang, X. Chen, N. S. Longo, M. Louder, K. McKee, S. O'Dell, S. Perfetto, S. D. Schmidt, W. Shi, L. Wu, Y. Yang, Z. Y. Yang, Z. Yang, Z. Zhang, M. Bonsignori, J. A. Crump, S. H. Kapiga, N. E. Sam, B. F. Haynes, M. Simek, D. R. Burton, W. C. Koff, N. A. Doria-Rose, M. Connors; NISC Comparative Sequencing Program, J. C. Mullikin, G. J. Nabel, M. Roederer, L. Shapiro, P. D. Kwong, J. R. Mascola, Focused evolution of HIV-1 neutralizing antibodies revealed by structures and deep sequencing. *Science* **333**, 1593–1602 (2011).
53. J. Zhu, S. O'Dell, G. Ofek, M. Pancera, X. Wu, B. Zhang, Z. Zhang; NISC Comparative Sequencing Program, J. C. Mullikin, M. Simek, D. R. Burton, W. C. Koff, L. Shapiro, J. R. Mascola, P. D. Kwong, Somatic populations of PGT135–137 HIV-1-neutralizing antibodies identified by 454 pyrosequencing and bioinformatics. *Front. Microbiol.* **3**, 315 (2012).
54. M. A. Larkin, G. Blackshields, N. P. Brown, R. Chenna, P. A. McGettigan, H. McWilliam, F. Valentin, I. M. Wallace, A. Wilm, R. Lopez, J. D. Thompson, T. J. Gibson, D. G. Higgins, Clustal W and Clustal X version 2.0. *Bioinformatics* **23**, 2947–2948 (2007).

Acknowledgments: We thank B. Hartman for technical assistance with figures; D. Ambrozak, A. Wheatley, and S. Narpala for technical assistance and thoughtful discussions; K. Tomioka, R. Kruthers, R. Plishka, and A. Buckler-White for determining plasma viral RNA loads; and B. Skopets, W. Magnanelli, and R. Petros for diligently assisting in the maintenance of animals and assisting with procedures. We also thank J. Binley (Torrey Pines Research Institute), D. Gabuzda (Dana-Farber Cancer Institute), D. Montefiori (Duke University Medical Center), M. Seaman (Beth Israel Deaconess Medical Center), and the NIH AIDS Reagent Program for Env plasmids used in the HIV-1 neutralization assays. **Funding:** This work was supported in part with federal funds from the National Cancer Institute, NIH, under contract HHSN261200800001E, by the Intramural Research Program of the Vaccine Research Center, the Intramural Research Program of the NIAID, NIH, and Collaboration for AIDS Vaccine Discovery grant no. OPP1032325 from the Bill and Melinda Gates Foundation (R.A.K.). **Author contributions:** T.Y., R.M.L., Y.N., J.R.M., M.A.M., and R.A.K. designed the research studies. T.Y., R.M.L., RG., R.M.-N., S.D.S., K.L.B., B.F.K., P.W., Z.S., and Y.N. performed the research and analyzed the data. S.D., C.P., A.B.M., R.A.S., L.S., and D.C.D. contributed reagents/materials/analysis tools. T.Y., R.M.L., Y.N., J.R.M., M.A.M., and R.A.K. wrote the paper. **Competing interests:** The authors declare that they have no competing financial interests. **Data and materials availability:** RM V_H sequences were deposited in GenBank with accession nos. KP710506 to KP71083. Env sequences were deposited in GenBank with accession nos. KM082157 to KM082524. BCR sequences were deposited in GenBank with accession nos. KM097097 to KM097988.

Submitted 21 April 2015
Accepted 19 June 2015
Published 29 July 2015
10.1126/scitranslmed.aab3964

Citation: T. Yamamoto, R. M. Lynch, R. Gautam, R. Matus-Nicodemos, S. D. Schmidt, K. L. Boswell, S. Darko, P. Wong, Z. Sheng, C. Petrovas, A. B. McDermott, R. A. Seder, B. F. Keele, L. Shapiro, D. C. Douek, Y. Nishimura, J. R. Mascola, M. A. Martin, R. A. Koup, Quality and quantity of T_{FH} cells are critical for broad antibody development in $SHIV_{AD8}$ infection. *Sci. Transl. Med.* **7**, 298ra120 (2015).

Science Translational Medicine

Quality and quantity of T_{FH} cells are critical for broad antibody development in $SHIV_{AD8}$ infection

Takuya Yamamoto, Rebecca M. Lynch, Rajeev Gautam, Rodrigo Matus-Nicodemos, Stephen D. Schmidt, Kristin L. Boswell, Sam Darko, Patrick Wong, Zizhang Sheng, Constantinos Petrovas, Adrian B. McDermott, Robert A. Seder, Brandon F. Keele, Lawrence Shapiro, Daniel C. Douek, Yoshiaki Nishimura, John R. Mascola, Malcolm A. Martin and Richard A. Koup

Sci Transl Med **7**, 298ra120298ra120.
DOI: 10.1126/scitranslmed.aab3964

How antibodies mature

Antibodies are stalwart protectors against infection, but even antibodies need a little help to do their jobs. T follicular helper (T_{FH}) cells can guide B cells to produce antibodies with improved specificity to a particular pathogen through a process called affinity maturation. Now, Yamamoto *et al.* report that in nonhuman primates, the frequency and quality of T_{FH} cells were associated with the development of broadly neutralizing antibodies that may be protective against SHIV. These findings suggest that HIV vaccines that incorporate T_{FH} cell stimulation may boost broadly neutralizing antibody production.